Separation Science and Technology
Publication details, including instructions for authors and subscription information:
http://www.informaworld.com/smpp/title~content=t713708471

Prediction of Solubility of Cholesterol in Supercritical Solvents

Seyed Foad Aghamiri[a]; Zahra Nickmand[a]
[a] Chemical Engineeing Department, Faculty of Engineering, University of Isfahan, Isfahan, Iran

To cite this Article Aghamiri, Seyed Foad and Nickmand, Zahra(2010) 'Prediction of Solubility of Cholesterol in Supercritical Solvents', Separation Science and Technology, 45: 14, 2119 — 2129
To link to this Article: DOI: 10.1080/01496395.2010.504448
URL: http://dx.doi.org/10.1080/01496395.2010.504448

Separation Science and Technology, 45: 2119–2129, 2010
Copyright © Taylor & Francis Group, LLC
ISSN: 0149-6395 print/1520-5754 online
DOI: 10.1080/01496395.2010.504448

Taylor & Francis
Taylor & Francis Group

Prediction of Solubility of Cholesterol in Supercritical Solvents

Seyed Foad Aghamiri and Zahra Nickmand
Chemical Engineeing Department, Faculty of Engineering, University of Isfahan, Isfahan, Iran

In this study the solubility of cholesterol was calculated in two supercritical pure solvents (carbon dioxide and ethane) as binary systems, and four supercritical solvent/co-solvent systems as ternary systems (cholesterol/carbon dioxide/methanol, cholesterol/ethane/acetone, cholesterol/ethane/hexane, cholesterol/ethane/propane) in various temperatures by SRK, PR, and SAFT equations of state. Pure molecular parameters of SAFT equation of state were obtained by fitting vapor pressure and liquid density data. Also the molecular parameters of cholesterol were obtained by fitting the solubility data of binary systems in one temperature, then they were used for the same system in other temperatures and for ternary systems with the same solvent. Results show that the SAFT equation of state can predict the trend and amount solubility of cholesterol in supercritical solvents much better than the other equations of state.

Keywords carbon dioxide; equation of state; SAFT model; supercritical fluid

INTRODUCTION

Supercritical fluid extraction (SCFE) is an efficient, simple, and safe process for separation, extraction, purification, and re-crystallization of solids in many industries such as foods, polymers, bio-chemicals, and pharmaceuticals industries (1,2). The solubility of solids will be increased proportional to the density of the solvent near the solvent's critical point. Supercritical fluids (SCFs) are increasingly replacing the organic solvents that are used in chemical industries for separating the heavy and valuable components (2). Equations of state are the most suitable models for predicting the solubility of solids in SCFs because these processes deal with high-pressure phase equilibria. Both cubic and noncubic equations of state have been used by researchers to this purpose (3,4). A comprehensive study has been carried out on the capability of the cubic equations of state to model the solubility of solids in SCFs by Ashour et al. (5). They concluded that no single cubic equation of state currently exists that is equally suitable for the quantitative prediction of all SCF mixtures. Economou et al. (6) used the SAFT equation of state to calculate the solubility of solid polynuclear aromatic hydrocarbons (PNA's) in supercritical ethylene and supercritical ethane (6).

Zhong and Yang combined the SAFT equation of state with eight different mixing rules to evaluate the ability of this approach for modeling the solubility of solids in supercritical fluids (SCFs). Results showed that the SAFT equation of state with one or two parametric mixing rules represented good correlative accuracy, which is comparable to that of cubic equations of state with three parametric mixing rules (7). Huang et al. (8) employed the perturbed Lennard–Jones chain (PLJC) equation to model the solubility of 39 solids in supercritical carbon dioxide. They used PLJC with three temperature independent parameters and the results showed superior ability of PLJC than PR equation of state with three temperature dependent parameters (8).

There exist a number of experimental works in the literatures to measure the solubility of solids in SCF. Adrian et al. (9) reported experimental results for the partitioning of small amounts of six biomolecules (adenine, caffeine, methyl anthranilate, L-phenylalanine, salicyl alcohol, and vanillin) on coexisting liquid phases in high-pressure three-phase vapor-liquid-liquid equilibrium of the ternary system "near critical" carbon dioxide + water + 1-propanol at 313 and 333 K. They correlated the experimental results for the partition coefficients with a semi-empirical approach, which combines an equation of state for describing the high-pressure multiphase equilibrium and the UNIQUAC excess Gibbs energy equation for describing the partitioning of the bio-molecules (9). Also in another work, Huang et al. (2004) measured the solubility of cholesterol and its esters-cholesteryl acetate, cholesteryl butyrate, and cholesteryl benzoate in supercritical carbon dioxide. Also, they correlated solubility data using the Peng-Robinson equation of state (PR equation of state) and density-based correlations (10). Matias et al. (11) measured the equilibrium solubility of coenzyme Q10 (CoQ10) in supercritical carbon dioxide ($scCO_2$) by a static analytical method in the pressure range

---

Received 16 September 2009; accepted 20 April 2010.

Address correspondence to Seyed Foad Aghamiri, Department of Chemical Engineering, Faculty of Engineering, University of Isfahan, Isfahan 8174673441, Iran. E-mail: aghamiri@petr.ui.ac.ir

from 9 to 26 MPa and at temperatures of 305, 313, and 323 K and investigated the co-solvent effect of ethanol in the solubility of the bioactive compound in supercritical carbon dioxide ($scCO_2$). They correlated the solubility data results by using the empirical density-based Chrastil model. Coimbra et al. (3) correlated the solubility of flurbiprofen, ketoprofen, naproxen, and ibuprofen in $scCO_2$ by using PR, SRK, PTV equations of state. Also, they employed van der Waals (vdW), Panagiotopoulos–Reid (mrPR), and Mukhopadhyay-Rao (MR) mixing rules, and several different sets of solid properties had been estimated (3), Darrell et al. (12) evaluated density-based, semi-empirical models in order to accurately correlate the solid solubility in supercritical carbon dioxide for six binary systems (solid + $scCO_2$) at three different isotherms. Shin et al. (13) measured the bubble points of dichloromethane + $scCO_2$ system at temperature from 303.2 to 328.2 K and the cloud points of polyvinylpyrrolidone (PVP) + dichloromethane + $scCO_2$ system at temperature ranging from 313.13 to 363.33 K and pressure up to 25.5 MPa. They correlated the phase behavior of experimental data satisfactorily with the quasi-chemical nonrandom lattice fluid (QLF) equation of state by introducing temperature-dependent binary interaction parameters. Park et al. 2009 (14) investigated the equilibrium solubility of two biocides, climbazole, and triclocarban, in supercritical carbon dioxide with static method in the pressure range from 10 to 40 MPa and at temperatures 313.2, 323.2, and 333.2 K. They correlated the experimental data by the Peng-Robinson equation of state and quasi-chemical nonrandom lattice fluid model (14).

SOLID–SCF CALCULATIONS

Solubility or solute mole fraction (y_i) in a supercritical fluid can be predicted by the equality of the fugacity of solute in condensed and supercritical phases, as follows (15):

$$y_i = \frac{P_i^{sat}}{P} \frac{\widehat{\phi}_i^{s}}{\widehat{\phi}_i^{V}} \exp\left(\frac{PV_i^s}{RT}\right) \tag{1}$$

Where P, P_i^{sat}, V_i^s, $\hat{\phi}_i^s$, $\hat{\phi}_i^V$, and T are respectively equilibrium pressure, saturated sublimation pressure of solute, pure solid molar volume, the fugacity coefficient in condensed phase, fugacity coefficient in vapor phase, and temperature. Since P_i^{sat}, is usually very small, the fugacity coefficient in condensed phase can be assumed to be unit, $\widehat{\phi}_i^{s} = 1$. Also the fugacity coefficient of the vapor phase, $\widehat{\phi}_i^{V}$, can be derived from an equation of state as follows:

$$RT \ln \widehat{\phi}_1^{v} = \int_V^{\infty} \left[\left(\frac{\partial P}{\partial n_i}\right)_{T,V,n_{j\neq i}} - \frac{RT}{V} \right] dV - RT \ln(Z) \tag{2}$$

In what follows the SAFT equation of state and two well known cubic equations of state will be introduced. These equations of state are used in this study to calculate the fugacity coefficients of solute in vapor phase. By using these equations the solubility of cholesterol in SCFs will be calculated.

SAFT Equation of State

Numerous models have been improved to take into account both physical and chemical interactions in non-ideal solutions. One of these successful models is statistical associating fluid theory (SAFT) (16). SAFT is a statistical mechanical equation of state developed from Wertheim's first-order perturbation theory. According to this theory, the residual molar Helmholtz free energy (a^{res}) is the sum of four terms considering different intermolecular forces (6,7,16):

$$a^{res} = a^{hs} + a^{disp} + a^{chain} + a^{assoc} \tag{3}$$

The first two terms (a^{hs} and a^{disp}) represent segment-segment interactions which are short-range repulsions and long-rang dispersion forces, the third term is added to take into account chain formation, and finally the fourth term considers molecular association. In this study the Carnahan-Starling (16) has been used as the reference fluid (a^{hs}), the dispersion term (a^{disp}) has been taken from Cotterman et al. (16), Chain formation contribution (a^{chain}) has been given by Chapman et al. (16) and Wertheim's theory has been used for a^{assoc}. This equation with the above-mentioned contributions is introduced in the appendix. The SAFT model has three molecular parameters for pure non-associating fluid: The number of segments per molecule, m, potential well depth, ϵ, and diameter of the segment, σ. For pure associating components there are two more parameters: association energy, ε^{AB}, and specific interactions between association sites on each molecule, K^{AB}. These parameters can be estimated from the fitting of saturated vapor pressure and liquid density data. The fugacity coefficient ($\emptyset_i$) for component i in the mixture according to the SAFT equation of state can be obtained as follows:

$$RT \ln \emptyset_i = \mu_i^{res} - RT \ln Z \tag{4}$$

Where μ_i^{res} is the residual chemical potential of component i and Z is the compressibility factor of the mixture. This equation is given in the appendix.

Cubic Equations of State

The general form of cubic equations of state is as follows (15):

$$P = \frac{RT}{V - b} - \frac{a(T)}{(V + \in b)(V + \delta b)} \tag{5}$$

Where a(T), $\in$, and δ have been listed in Table 1 for used equations in this study.

TABLE 1
Cubic equations of state used in this study

Name	δ	ε	Ω	a (T)
Soave–Redlich–Kwong (SRK)	1	0	0.08664	$\mathrm{a(T)} = 0.42747\frac{R^2T_c^2}{P_c} \times \propto (T_r, \omega)$ $\alpha(T_r, \omega) = [1 + m(1 - \sqrt{T_r})]^2$ $m = 0.480 + 1.574\,\omega - 0.176\,\omega^2$
Peng–Robinson (PR)	$1 + \sqrt{2}$	$1 - \sqrt{2}$	0.07779	$\mathrm{a(T)} = 0.45724\frac{R^2T_c^2}{P_c} \times \propto (T_r, \omega)$ $\alpha(T_r, \omega) = [1 + K(1 - \sqrt{T_r})]^2$ $K = 0.37464 + 1.54226\,\omega - 0.26992\,\omega^2$

TABLE 2
Properties of components used in this study

Compound	T_c (K)	P_c (bar)	v^s (L/mol)	Ref.
Acetone	508.2	47.01		(15)
Carbon dioxide (CO_2)	304.12	73.74		(15)
Cholesterol ($C_{27}H_{46}O$)	778.70	12.20	0.3624	(18)
Ethane (C_2H_6)	305.42	48.80		(15)
Hexane (C_6H_{14})	507.60	30.25		(15)
Methanol (CH_3OH)	512.60	80.97		(15)
Propane (C_3H_8)	369.80	42.48		(15)

According to Eq. (2) the following expression for the fugacity coefficient of component i in the mixture will be obtained:

$$\ln \widehat{\phi}_i = \frac{b_i}{b}(Z - 1) - \ln(Z - \beta) - \overline{q_i}I \tag{6}$$

Where

$$Z_i = 1 + \beta_i - q_i\beta_i \frac{Z_i - \beta_i}{(Z_i + \in \beta_i) + (Z_i + \delta\beta_i)} \tag{7}$$

$$b_i = \Omega\frac{RT_{ci}}{P_{ci}} \tag{8}$$

$$a_i = \psi\frac{R^2T_{ci}^2}{P_{ci}}\alpha(T_{ri}, W) \tag{9}$$

$$q_i = \frac{a_i(T)}{b_iRT} \tag{10}$$

$$\beta = \frac{bP}{RT} \tag{11}$$

$$a = \sum_i\sum_j y_iy_ja_{ij} \tag{12}$$

$$a_{ij} = (1 - k_{ij})(a_ia_j)^{1/2} \quad \text{for } i = j \quad k_{ij} = 0 \tag{13}$$

$$b = \sum_i y_ib_i \tag{14}$$

$$\bar{q}_t\left[\frac{\partial(nq)}{\partial n_i}\right]_{T,n_j} \tag{15}$$

TABLE 3
Pure molecular parameters of SAFT equation of state

Components	T(K)	n_d	m	ε/k (K)	σ (Å)	ε^{ABa}	K^{ABa}	ΔP^b	$\Delta\rho^b$
Acetone	283–473	6	3.186	214.539	3.160	–	–	0.818	2.531
Carbon dioxide	220–280	6	3.000	324.063	5.322	–	–	0.068	1.005
Ethane	150–260	5	1.574	181.370	3.591	2231.249	0.000001	0.166	1.137
Hexane	278–450	5	3.427	203.621	3.700	–	–	0.839	1.329
Methanol	301.7–356	3	1.637	243.557	3.539	2246.309	0.01392	0.254	3.000
Propane	283.15–483.15	6	2.095	187.420	3.604	–	–	0.097	0.713

[a] These parameters are zero for non-associating fluids.

[b] $\Delta P = \frac{100}{n_d} \times \sum_{k=1}^{n_d}\left(\left|\frac{P^{exp} - P^{cal}}{P^{exp}}\right|\right)_k$, $\Delta\rho = \frac{100}{n_d} \times \sum_{k=1}^{n_d}\left(\left|\frac{P^{exp} - P^{cal}}{P^{exp}}\right|\right)_k$.

TABLE 4
Pure molecular parameters of SAFT equation of state for cholesterol obtained by fitting of binary experimental data[a]

System	T (K)	n_d	m	ϵ/k (K)	σ (Å)
Cholesterol+Carbon dioxide	323.15	6	3	159.8141	6.0270
Cholesterol+Ethane	323.15	7	3	324.0627	5.3221

[a] $O.F. = \frac{1}{n_d} \times \sum_{i=1}^{n_d} |y_i^{exp} - y_i^{cal}|$.

TABLE 6
Binary interaction parameters of binary systems

			k_{12}		
System	T (K)	n_d	SRK	PR	SAFT
1[a]	313.15	6	−0.095	−0.022	−0.002
	323.15	6	−0.094	−0.012	1.3e-8
	333.15	5	−0.081	−0.007	0.002
2[b]	313.15	8	−0.136	0.086	−6.39e-4
	323.15	8	−0.139	0.091	−4.70e-4
	333.15	7	−0.135	0.095	4.27e-4

[a] Cholesterol/Carbon dioxide.
[b] Cholesterol/Ethane.

$$l = \frac{1}{\delta - \in} \ln \frac{z + \delta\beta}{z + \epsilon\beta} \tag{16}$$

The critical properties of the compounds involved in this study are given by Table 2.

In the next section solubility of cholesterol in pure and mixtures of SCFs have been calculated by SAFT, SRK, and PR equations of state.

RESULTS AND DISCUSSION

Estimation of SAFT Parameters

The vapor pressure and liquid density data have been used to obtain molecular parameters of SAFT for pure solvents used in this study (m, ϵ, σ, ϵ^{AB}, K^{AB}), by minimizing the following objective function:

$$O.F. = \frac{100}{n_d} \times \sum_{k=1}^{n_d} \left(\left| \frac{P^{exp} - P^{cal}}{P^{exp}} \right| + \left| \frac{\rho^{exp} - \rho^{cal}}{\rho^{exp}} \right| \right)_k \tag{17}$$

Where P, ρ, and n_d are vapor pressure, liquid density, and number of data, respectively. Also, *exp.* and *cal.* in superscripts denote experimental and calculated data respectively. Experimental data have been taken from reference (17). Results for pure molecular parameters have been given by Table 3. Also, in this table have been reported the relative deviation for prediction of vapor pressure and liquid density, ΔP and $\Delta\rho$, respectively. Due to lack of PVT experimental data for pure cholesterol, the molecular parameters of this compound were obtained by fitting binary experimental solubility data introduced in next section.

Prediction of Solubility of Cholesterol in Supercritical Solvents

In this section the solubility of cholesterol has been calculated in pure supercritical solvents (CO_2 and C_2H_6) and four systems in which acetone, hexane, propane, and methanol are used as co-solvents with carbon dioxide or ethane. All calculations have been done by using three

TABLE 5
Calculated absolute deviation for solubility of cholesterol by SAFT, SRK, and PR equations of state for two binary solid-SCF systems

		With $k_{ij}=0$			With $k_{ij} \neq 0$			
		AD[c]			AD[c]			
System	T (K)	SRK	PR	SAFT	SRK	PR	SAFT	Ref.
1[a]	313.15	5.383e-5	4.676e-5	5.186e-6	2.946e-5	2.661e-5	2.602e-6	(19)
	323.15	5.738e-5	4.042e-5	6.250e-7	2.741e-5	2.521e-5	6.231e-7	(19)
	333.15	6.884e-5	3.550e-5	4.653e-6	3.139e-5	2.889e-5	3.087e-6	(19)
2[b]	313.15	1.200e-4	0.087	4.824e-6	2.946e-5	2.419e-5	3.859e-6	(20)
	323.15	1.352e-4	0.072	5.974e-6	2.979e-5	2.488e-5	5.951e-6	(20)
	333.15	1.629e-4	0.064	3.475e-6	3.012e-5	2.540e-5	2.798e-6	(20)

[a] Cholesterol/Carbon dioxide.
[b] Cholesterol/Ethane.
[c] $AD = \frac{1}{n_d} \times \sum_{i=1}^{n_d} |y_i^{exp} - y_i^{cal}|$.

equations of state (SRK, PR, and SAFT). Table 4 introduces SAFT parameters for cholesterol obtained by fitting the binary solubility experimental data of cholesterol/carbon dioxide and cholesterol/ethane both at 323.15 K. According to this table, calculated parameters are different for two systems and this shows the effect of the solvent on the estimated molecular parameters of SAFT equation of state. These parameters have been used to predict the solubility of cholesterol in the same solvent at other temperatures and in solvent/co-solvent systems with a similar solvent.

The pure molecular parameters of SAFT equation of state for cholesterol with the binary interaction parameters (k_{12}) for three equations of state have been obtained by minimizing the following objective function:

$$O.F. = \frac{1}{n_d} \times \sum_{i=1}^{n_d} |y_i^{exp} - y_i^{cal}| \tag{18}$$

Where n_d, y_i^{exp}, and y_i^{cal} are the number of experimental data, experimental solubility data, and calculated solubility data, respectively.

The solubility of cholesterol in supercritical carbon dioxide has been predicted by SRK, PR, and SAFT equations of state for three isotherms (313.15, 323.15, and 333.15 K). Table 5 shows the absolute deviation (AD) in prediction of solubility data corresponding to the above mentioned temperatures, for all equations of state. Also, the optimized interaction parameters for this system (calculated by Eq. 18) have been reported in Table 6 for three equations of state. According to this table, the absolute values of corresponding k_{ij} of SAFT equation of state for three isotherms are smaller than those of the other two equations of state. Results of the solubility of cholesterol in supercritical carbon dioxide at temperature of 313.15 K have been presented in Fig. 1. This figure shows the results of three equations of state with $k_{ij} = 0$ and $k_{ij} \neq 0$. According to this figure the SAFT model is in good agreement with experimental data specifically at high pressures with $k_{ij} = 0$ and $k_{ij} \neq 0$, and shows the correct trend with experimental data, while PR and SRK equations of state significantly deviate from experimental data at high pressures. The solubility versus pressure behavior for this system at T = 323.15 and 333.15 K, are similar to that of T = 313.15 K, for PR, SRK, and SAFT equations of state.

Solubility of cholesterol in supercritical ethane has been predicted by three equations of state for three different isotherms. The absolute deviation (AD) and the optimized interaction parameters for cholesterol/ethane system have been reported in Tables 5 and 6 respectively. Table 5 shows that for two cases ($k_{ij} = 0$ and $k_{ij} \neq 0$) the absolute deviation for the SAFT model is too much smaller than the other equations of state. As can be seen in Table 6, the binary interaction

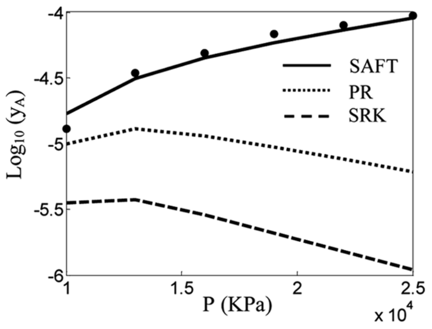

(a) $k_{ij} = 0$

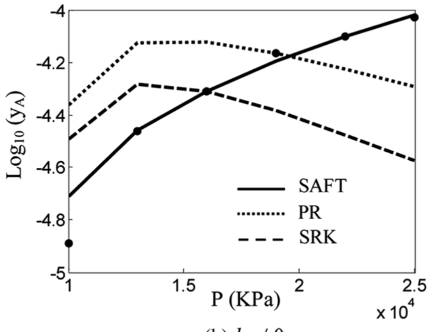

(b) $k_{ij} \neq 0$

FIG. 1. Log_{10} of solubility of cholesterol in supercritical carbon dioxide at T = 313.15 K. ● are the experimental data, ___ is SAFT, ... is PR, and -- is SRK.

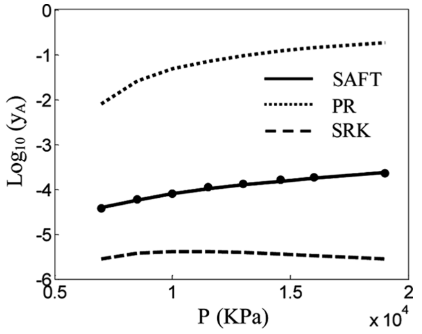

(a) $k_{ij} = 0$

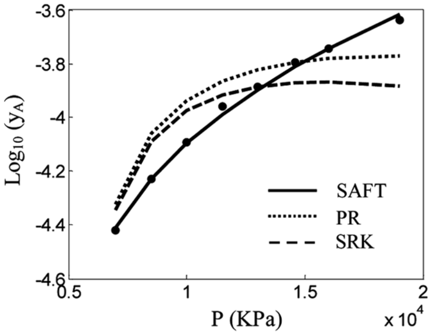

(b) $k_{ij} \neq 0$

FIG. 2. Log_{10} of solubility of cholesterol in supercritical ethane at T = 313.15 K. ● are the experimental data, ___ is SAFT, ... is PR, and -- is SRK.

TABLE 7
Calculated absolute deviation (AD) for solubility of cholesterol by SAFT, SRK, and PR equations of state for four ternary systems

System				AD[a]			AD			
				With $k_{ij}=0$			With $k_{ij}\neq 0$			
1	2	3	T (K)	SRK	PR	SAFT	SRK	PR	SAFT	Ref.
Cholesterol	Ethane	Acetone	318.15	3.113e-4	0.871	8.010e-5	3.796e-5	3.717e-5	3.850e-6	(20)
			328.15	3.611e-4	0.988	6.519e-5	2.457e-5	2.528e-5	1.364e-5	(20)
			338.15	4.666e-4	0.983	1.362e-4	2.056e-5	2.417e-5	1.291e-5	(20)
Cholesterol	Ethane	Propane	318.15	1.672e-4	1.009	3.919e-5	1.957e-5	1.484e-5	3.944e-6	(20)
			328.15	2.205e-4	1.072	4.534e-5	1.458e-5	1.609e-5	2.062e-6	(20)
Cholesterol	Ethane	Hexane	328.15	2.471e-4	1.542	3.263e-5	2.725e-5	2.774e-5	4.700e-6	(20)
			338.15	3.084e-4	1.553	2.662e-5	2.024e-5	2.163e-5	7.982e-6	(20)
Cholesterol	Carbon dioxide	Methanol	308.20	2.420e-4	2.393e-4	2.144e-4	5.892e-5	4.815e-5	8.134e-6	(21)

[a] $AD = \frac{1}{n_d} \times \sum_{i=1}^{n_d} |y_i^{exp} - y_i^{cal}|$.

TABLE 8
Binary interaction parameters for ternary systems of Table 7

System				Parameters								
				SRK			PR			SAFT		
1	2	3	n_d	k_{12}	k_{13}	k_{23}	k_{12}	k_{13}	k_{23}	k_{12}	k_{13}	k_{23}
Cholesterol	Ethane	Acetone	7	−0.095	−0.788	0.591	0.008	3.252	1.634	−0.010	0.001	0.139
			6	0.319	−6.397	0.619	−0.287	7.403	1.642	−0.008	0.001	0.177
			6	−0.149	−0.237	0.732	0.432	−2.544	1.713	−0.015	0.0001	0.169
Cholesterol	Ethane	Propane	7	−0.120	−0.355	0.872	0.369	−2.188	2.522	−0.005	−0.053	0.413
			6	−0.138	−0.001	1.308	0.530	−5.297	2.595	−0.006	−0.056	0.318
Cholesterol	Ethane	Hexane	7	−0.149	−0.002	0.353	0.345	−1.053	1.262	0.001	−0.063	0.110
			6	−0.157	0.077	0.361	0.206	0.496	1.223	−0.005	0.014	0.079
Cholesterol	Carbon dioxide	Methanol	7	−0.138	0.617	1.146	0.266	−0.584	2.480	−0.055	0.013	0.029

parameters of the SAFT model are very small in comparison with SRK and PR equations of state. In these calculations obtained pure molecular parameters of SAFT model at T = 323.15 K have been used for other temperatures.

Figure 2 shows the solubility of cholesterol in supercritical ethane at temperature 313.15 K. According to this figure, the results of the SAFT equation of state are in superior agreement with the experimental data.

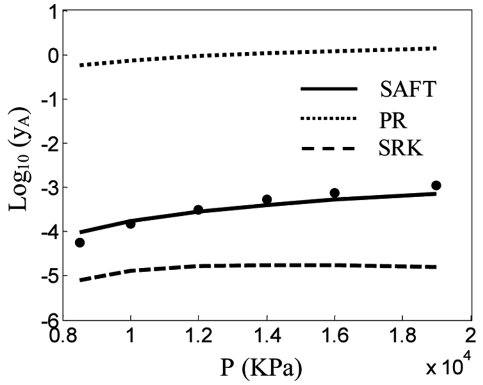

(a) $k_{ij} = 0$

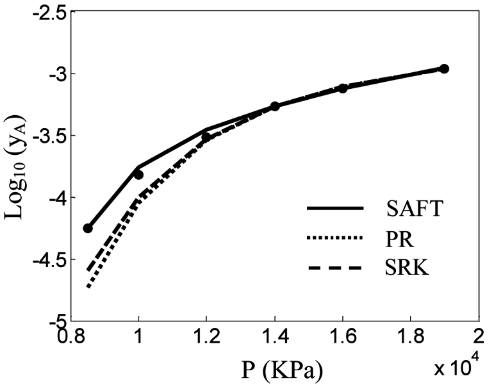

(b) $k_{ij} \neq 0$

FIG. 3. Log_{10} of solubility of cholesterol in supercritical ethane and acetone at T = 338.15 K. ● are the experimental data, ___ is SAFT, ... is PR, and - - is SRK.

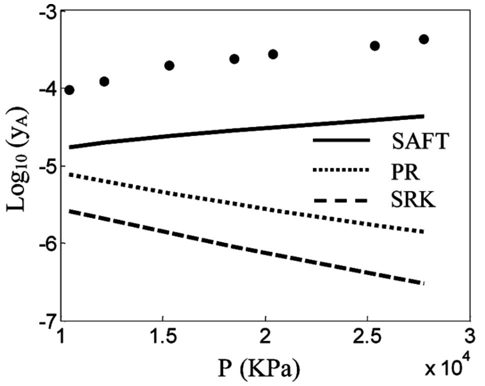

(a) $k_{ij} = 0$

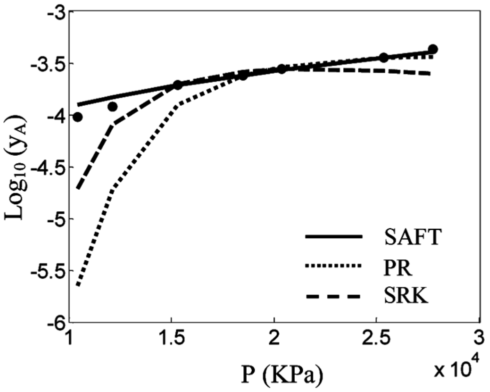

(b) $k_{ij} \neq 0$

FIG. 4. Log_{10} of solubility of cholesterol in supercritical carbon dioxide and methanol at T = 308.2 K. ● are the experimental data, ___ is SAFT, ... is PR, and - - is SRK.

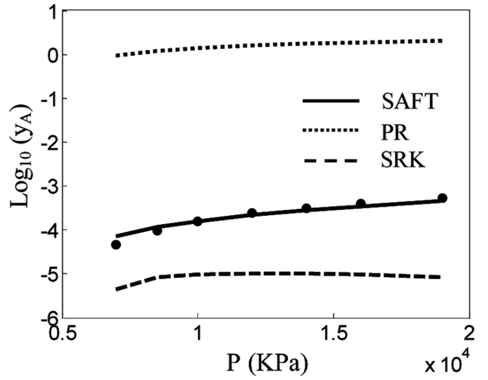

(a) $k_{ij} = 0$

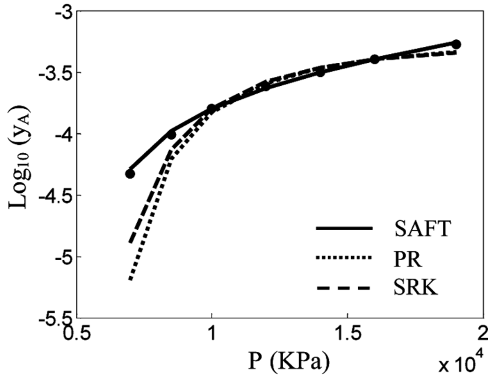

(b) $k_{ij} \neq 0$

FIG. 5. Log$_{10}$ of solubility of cholesterol in supercritical ethane and hexane at T = 328.15 K. ● are the experimental data, ___ is SAFT, ... is PR, and - - is SRK.

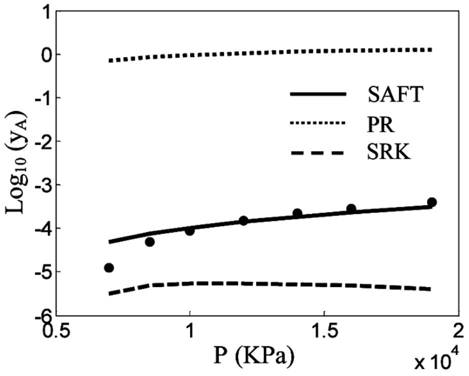

(a) $k_{ij} = 0$

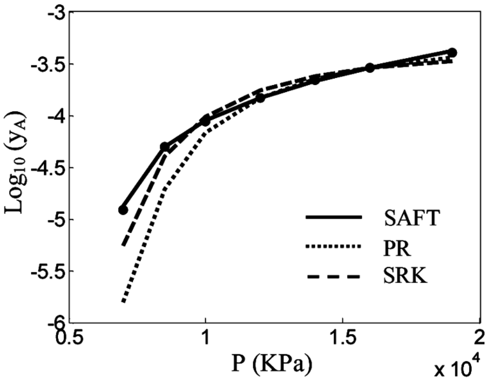

(b) $k_{ij} \neq 0$

FIG. 6. Log$_{10}$ of Solubility of cholesterol in supercritical ethane and propane at T = 318.15 K. ● are the experimental data, ___ is SAFT, ... is PR, and - - is SRK.

The solubility versus pressure behavior for this system at T = 323.15 and 333.15 K, are as same as T = 313.15 K, for all equations of state.

The obtained results for solubility of cholesterol in four solvent/co-solvent mixture have been given in Table 7 at different temperatures. This table indicates that SAFT can predict solubility in a more accurate way to experimental data compared with SRK and PR for all systems in studied cases ($k_{ij} = 0$ and $k_{ij} \neq 0$). Pure molecular parameters of the SAFT model shown in Tables 3 and 4 have been used for these calculations. Also, three binary interaction parameters have been obtained for three equations of state and reported in Table 8. Similar to binary systems, binary interaction parameters of the SAFT model for these ternary systems are very small, while those of SRK and PR equations of state are not.

Figure 3 shows the calculated solubility of cholesterol in supercritical ethane/acetone system at 338.15 K. As can be seen the best results have been achieved by using the SAFT equation of state for this isotherm. The obtained figures for the behavior of solubility versus pressure at T = 318.15 and 328.15 K are as same as T = 338.15 K.

Solubility of cholesterol in supercritical carbon dioxide and methanol as co-solvent has been depicted in Fig. 4 at T = 308.2 K. For this system prediction of the SAFT model is better than the other two equations of state.

Figure 5 is associated with the obtained results by three equations of state for solubility of cholesterol in supercritical ethane and hexane as co-solvent at T = 328.15 K. Results of comparison show that similar to other systems, predictions of the SAFT model for solubility of cholesterol in supercritical solvent is very well. We can observe the same figure for T = 338.15 K.

Also Fig. 6 shows the solubility of cholesterol in supercritical ethane with propane as co-solvent at T = 318.15 K, respectively. According to this figure the SAFT model produces more accurate results for both $k_{ij} = 0$ and $k_{ij} \neq 0$ in comparison with the other two equations of state. According to other systems the figure of solubility versus pressure at T = 328.15 K is similar to T = 318.15 K.

CONCLUSION

In this study we investigated the solubility of cholesterol in two supercritical pure solvent and four supercritical solvent/co-solvent systems at various temperatures. Calculations of solubility of cholesterol have been done in two cases: $k_{ij} = 0$ and $k_{ij} \neq 0$ by SRK, PR, and SAFT equations of state. According to the results, the SAFT model is preferable for predicting the solubility of cholesterol in supercritical solvents. Also, the SAFT model is able to predict the solubility of cholesterol in solvent/co-solvent systems by using the molecular parameters of cholesterol obtained from pure solvent experimental data.

ACKNOWLEDGEMENTS

This research was fully supported by the grant from the research deputy of University of Isfahan (Grant NO. 861233)

LIST OF SYMBOLS

a	molar Helmholtz energy (total, res, seg,, bond, assoc, etc.), per mole of molecules
a_0	segment molar Helmholtz energy (seg), per mole of segments
k	Boltzman's constant $\approx 1.381 \times 10^{-23}$ J/K
k_{ij}	binary interaction parameter between component i and j
$K^{A_iB_j}$	volume of interaction between site A on molecule i and site B on molecule j, dimensionless
m	the number of segments per molecule
n_d	number of data
N_{Av}	Avogadro's number $\approx 6.02 \times 10^{23}$molecules/mol
O.F.	objective function
P	pressure
P_i^{sat}	sublimation pressure of solute
R	gas constant
T	temperature
V_i^s	pure solid molar volume
x_i	mole fraction of component i
X^{Ai}	mole fraction of component i not bonded at site A
y_i	solubility of component i
Z	compressibility factor

Greek Letters

$\Delta^{A_iB_j}$	strength of interaction between site A on molecule i and site B on molecule j, Å^3
$\varepsilon^{A_iB_j}$	association energy of interaction between site A on molecule i and site B on molecule j, per molecule
μ_i^{res}	residual chemical potential of component i
ε	potential well depth
σ	Lenard-Jones segment diameter (temperature independent), Å
$\hat{\phi}_i^s$	fugacity coefficient in condensed phase
$\hat{\phi}_i^v$	fugacity coefficient in vapor phase

Superscripts

Assoc	association or due to association
Cal	calculated
Disp	dispersion
Exp	experimental
Hs	hard sphere
Ideal	ideal gas
Res	residual
Sat	saturated
Seg	segment

REFERENCES

1. Sarrade, S.; Guizard, C.; Rios, G.M. (2003) New applications of supercritical fluids and supercritical fluids processes in separation. *Sep. Purif. Technol.*, 32 (1–3): 57.
2. Brunner, G. (2005) Supercritical fluids: technology and application to food processing. *J. Food Eng.*, 67 (1–2): 21.
3. Coimbra, P.; Duarte, C.M.M.; de Sousa, H.C. (2006) Cubic equation-of-state correlation of the solubility of some anti-inflammatory drugs in supercritical carbon dioxide. *Fluid Phase Equilibr.*, 239 (2): 188.
4. de la Fuente, J.C.; Valderrama, J.O.; Bottini, S.B.; del Valle, J.M. (2005) Measurement and modeling of solubilities of capsaicin in high-pressure CO_2. *J. Supercrit. Fluids*, 34 (2): 195.
5. Ashour, I.; Almehaideb, R.; Fateen, S.-E.; Aly, G. (2000) Representation of solid-supercritical fluid phase equilibria using cubic equations of state. *Fluid Phase Equilibr.*, 167 (1): 41.
6. Economou, I.G.; Greggt, Ch.J.; Radosz, M. (1992) Solubilities of solid polynuclear aromatics (PNA's) in supercritical ethylene and ethane from statistical associating fluid theory (SAFT): Toward separating PNA's by size and structure. *Ind. Eng. Chem. Res.*, 31 (11): 2620.
7. Zhong, C.; Yang, H. (2002) Representation of the solubility of solids in supercritical fluids using the SAFT equation of state. *Ind. Eng. Chem. Res.*, 41 (19): 4899.
8. Huang, Z.; Kawi, S.; Chiew, Y.C. (2004) Application of the perturbed Lennard–Jones chain equation of state to solute solubility in supercritical carbon dioxide. *Fluid Phase Equilibr.*, 216 (1): 111.
9. Adrian, T.; Freitag, J.; Maurer, G. (2000) Partitioning of some biomolecules at high pressures to aqueous/organic liquid–liquid phases of the carbon dioxide+water+1-propanol system. *J. Supercrit. Fluids*, 17 (3): 197.
10. Huang, Z.; Kawi, S.; Chiew, Y.C. (2004) Solubility of cholesterol and its esters in supercritical carbon dioxide with and without cosolvents. *J. Supercrit. Fluids*, 30 (1): 25.
11. Matias, A.A.; Nunes, A.V.M.; Casimiro, T.; Duarte, C.M.M. (2004) Solubility of coenzyme Q10 in supercritical carbon dioxide. *J. Supercrit. Fluids*, 28 (2–3): 201.
12. Sparks, D.L.; Hernandez, R.; Estevez, L.A. (2008) Evaluation of density-based models for the solubility of solids in supercritical carbon dioxide and formulation of a newmodel. *Chem. Eng. Sci.*, 63 (17): 4292.
13. Shin, M.S.; Lee, J.H.; Kim, H. (2008) Phase behavior of the poly (vinyl pyrrolidone)+dichloromethane+supercritical carbon dioxide system. *Fluid Phase Equilibr.*, 272 (1–2): 42.
14. Park, C.I.; Shin, M.S.; Kim, H. (2009) Solubility of climbazole and triclocarban in supercritical carbon dioxide: Measurement and correlation. *J. Chem. Thermodyn.*, 41 (1): 30.
15. Smith, J.M.; Van Ness, H.C.; Abbott, M.M. (2002) *Chemical Engineering Thermodynamics*, 6th Ed.; Mc Graw Hill: New York.
16. Chapman, W.G.; Gubbins, K.E.; Jackson, G.; Radosz, M. (1990) New Reference Equation of State for Associating Liquids. *Ind. Eng. Chem. Res.*, 29 (8): 1709.
17. Perry, R.H.; Green, D.W. (2007) *Chemical Engineer's Handbook*, 8th Ed.; McGraw-Hill: New York.

18. Hartono, R.; Mansoori, G.A.; Suwono, A. (2001) Prediction of solubility of biomolecules in supercritical solvents. *Chem. Eng. Sci.*, 56: 6949.
19. Singh, H.; Yun, S.L.J.; Macnaughton, S.J.; Tomasko, D.L.; Foster, N.R. (1993) Solubility of cholesterol in supercritical ethane and binary gas mixtures containing ethane. *Ind. Eng. Chem. Res.*, 32 (11): 2841.
20. Foster, N.R.; Singh, H.S.; Yun, S.L.J.; Tomasko, D.L.; Macnaughton S.J. (1993) Polar and nonpolar cosolvent effects on the solubility of cholesterol in supercritical fluids. *Ind. Eng. Chem. Res.*, 32 (11): 2849.
21. Wong, J.M.; Johnston, K.P. (1986) Solubilization of biomolecules in carbon dioxide based supercritical fluids. *Biotechnol. Progr.*, 2 (1): 29.

APPENDIX

Helmholtz Free Energy of SAFT Equation of State

According to Chapman et al. (16) the residual molar Helmholtz free energy (a^{res}) is the sum of four terms as follows (6,7,15):

$$a^{res} = a^{hs} + a^{disp} + a^{chain} + a^{assoc} \tag{A-1}$$

Hard Sphere Term

$$\frac{a^{hs}}{RT} = m\frac{4\eta - 3\eta^2}{(1-\eta)^2} \tag{A-2}$$

η is defined for pure components and mixtures as the following:

$$\eta = (\pi N_{A\nu}/6)\rho d^3 m \qquad \text{(Pure fluids)} \tag{A-3}$$

$$\eta = (\pi N_{A\nu}/6)\rho d^3 \sum\nolimits_i x_i m_i \qquad \text{(Mixtures)} \tag{A-4}$$

In equations (A-3) and (A-4), d is temperature-dependent hard sphere diameter:

$$d = \sigma f(kT/\varepsilon, m) \tag{A-5}$$

where:

$$f(kT/\varepsilon, m) = \frac{1 + 0.2977(kT/\varepsilon)}{1 + 0.33163(kT/\varepsilon) + f(m)(kT/\varepsilon)^2} \tag{A-6}$$

and

$$f(m) = 0.0010477 + 0.025337((m-1)/m) \tag{A-7}$$

Dispersion Term

$$\frac{a^{disp}}{RT} = \frac{m}{T_R}\left(a_{01}^{disp} + a_{02}^{disp}/T_R\right) \tag{A-8}$$

with the following definitions for a_{01}^{disp} and a_{02}^{disp}:

$$a_{01}^{disp} = \rho_R[-8.5959 - 4.5424\rho_R - 2.1268\rho_R^2 + 10.285\rho_R^3 \tag{A-9}$$

$$a_{02}^{disp} = \rho_R[-1.9075 - 9.9724\rho_R - 22.216\rho_R^2 + 15.904\rho_R^3 \tag{A-10}$$

also $T_R = kT/\varepsilon$ and $\rho_R = [6/(2^{0.5}\pi)]\eta$ are reduced temperature and density, respectively.

Chain Term

$$\frac{a^{chain}}{RT} = \sum\nolimits_i x_i(1 - m_i)\ln(g_{ii}(d_{ii})^{hs}) \tag{A-11}$$

In equation (A-11), $g_{ij}(d_{ij})^{seg}$ is radial distribution function for mixtures of hard spheres and defined as (16):

$$g_{ij}(d_{ij})^{seg} = \frac{1}{1-\xi_3} + \frac{3d_{ii}d_{jj}}{d_{ii}+d_{jj}}\frac{\xi_2}{(1-\xi_3)^2} + 2\left[\frac{d_{ii}d_{jj}}{d_{ii}+d_{jj}}\right]^2\frac{\xi_2}{(1-\xi_3)^3} \tag{A-12}$$

where

$$\xi_k = (\pi N_{A\nu}/6)\rho\sum\nolimits_i x_i m_i d_{ii}^k \quad k = 0, 1, 2, 3 \tag{A-13}$$

$g_{ij}(d_{ij})^{seg}$ is given by the following relation for a pure hard sphere fluid (16):

$$g(d)^{seg} = \frac{2-\eta}{2(1-\eta)^3} \tag{A-14}$$

Association Term

$$\frac{a^{assoc}}{RT} = \sum_A [lnX^A - X^A/2] + M/2 \quad \text{(Pure associating fluid)} \tag{A-15}$$

$$X^A = [1 + N_{AV}\sum\nolimits_B \rho X^B \Delta^{AB}]^{-1} \tag{A-16}$$

Δ^{AB} is the association strength for pure fluid and defined as Eq. (A-17):

$$\Delta^{AB} = d^3 \mathrm{g}(d)^{seg} K^{AB}[\exp(\varepsilon^{AB}/kT) - 1] \tag{A-17}$$

Also the association term for mixtures is defined as the following (16):

$$\frac{a^{assoc}}{RT} = \sum_i x_i\left[\sum_{Ai}[\ln \mathrm{X}^A - X^{Ai}/2]\right] + M_i/2$$

$$\text{(A mixture of associating fluids)} \tag{A-18}$$

$$X^{Ai} = [1 + N_{AV}\sum\nolimits_j\sum\nolimits_{Bj}\rho_j X^{Ai}\Delta^{A_iB_j}]^{-1} \tag{A-19}$$

where $\Delta^{A_iB_j}$, the association strength for mixtures, is given by the following Eq. (16):

$$\Delta^{A_iB_j} = d_{ij}^3 \mathrm{g}_{ij}(d_{ij})^{seg} K^{A_iB_j}[\exp(\varepsilon^{A_iB_j}/kT) - 1] \tag{A-20}$$

where

$$d_{ij} = (d_i + d_j)/2 \tag{A-21}$$

Regarding equations (A-1),(A-2), (A-8), (A-11), and (A-15) the residual Helmholtz free energy of SAFT for a pure fluid is obtained as follows (16):

$$\frac{a^{res}}{RT} = m\frac{4\eta - 3\eta^2}{(1-\eta)^2} + \frac{m}{T_R}(a_{01}^{disp} + a_{02}^{disp}/T_R) + (1-m)\ln(g(d)^{seg}) + \sum_A [lnX^A - X^A/2] + m/2] \tag{A-22}$$

Also Helmholtz free energy of SAFT for a mixture is obtained as Eq. (A-23) (16):

$$\frac{a^{res}}{RT} = m_x\frac{4\eta - 3\eta^2}{(1-\eta)^2} + \frac{m_x}{T_R}(a_{01}^{disp} + a_{02}^{disp}/T_R) + \sum_i x_i(1-m_i)ln(g_{ii}(d_{ii})^{hs}) + \sum_i x_i\left[\sum_{Ai}[lnX^A - X^{Ai}/2]\right] + M_i/2 \tag{A-23}$$

where m_x is approximated by (16):

$$m_x = \sum_i x_i m_i \tag{A-24}$$

also σ_x and ε_x are equivalent to σ and ε for mixtures and they can be calculated by the following mixing rules (16):

$$\sigma_x^3 = \frac{\sum_i\sum_j x_i x_j m_i m_j \sigma_{ij}^3}{(\sum_i x_i m_i)^2} \tag{A – 25}$$

$$\varepsilon_x\sigma_x^3 = \frac{\sum_i\sum_j x_i x_j m_i m_j \sigma_{ij}^3\varepsilon_{ij}}{(\sum_i x_i m_i)^2} \tag{A-26}$$

In the above equations the unlike-interaction energy parameter, ε_{ij}, is determined by a modified van der Waals one-fluid mixing rule (16):

$$\varepsilon_{ij} = k_{ij}(\varepsilon_{ii}\varepsilon_{jj})^{1/2} \tag{A-27}$$

Also the unlike-interaction size parameter, σ_{ij}, is determined by an arithmetic average (16):

$$\sigma_{ij} = (\sigma_{ii} + \sigma_{jj})/2 \tag{A-28}$$

Fugacity Coefficient

$$RT\ln\emptyset_i = \mu_i^{res} - RT\ln Z \tag{A-29}$$

where

$$Z = Z^{seg} + Z^{chain} + Z^{assoc} \tag{A-30}$$

and

$$Z^{seg} = 1 + (Z_0^{seg} - 1)\sum_i X_i m_i \tag{A-31}$$

$$Z_0^{seg} = Z_0^{hs} + Z_0^{disp} \tag{A-32}$$

$$Z_0^{hs} = \frac{1 + \eta + \eta^2 - \eta^3}{(1-\eta)^3} \tag{A-33}$$

$$Z_0^{disp} = \frac{Z_{01}^{disp}}{T_R} + \frac{Z_{02}^{disp}}{T_R{}^2} \tag{A-34}$$

$$Z_{01}^{disp} = \rho_R[-8.595 - 2(4.5452\rho_R) - 3(2.1268\rho_R^2) + 4(10.285\rho_R^3)] \tag{A-35}$$

$$Z_{02}^{disp} = \rho_R[-1.9075 - 2(9.9724\rho_R) - 3(22.216\rho_R^2) + 4(15.904\rho_R^3)] \tag{A-36}$$

$$Z^{chain} = \sum_i X_i(1-m_i)\rho\left[\frac{\delta\ln g_{ii}(d_{ii})^{hs}}{\delta\rho}\right]_{T,X_j} \tag{A – 37}$$

$$Z^{assoc} = \sum_i X_i\frac{Z_i^{assoc}}{RT} - \frac{a^{assoc}}{RT} \tag{A – 38}$$

also

$$\mu_i^{res} = \mu_i^{seg} + \mu_i^{chain} + \mu_i^{assoc} \tag{A – 39}$$

where

$$\mu_i = \frac{\partial}{\partial n_i}\left(\frac{a}{RT}\right) \tag{A – 40}$$